A new zinc (II) responsive MRI contrast agent

Adhitiyawarman[1,2] and Mark P. Lowe[2]*
1. Department of Chemistry, Faculty of Mathematics and Natural Sciences, University of Tanjungpura, Jl. Prof. Dr. H. Hadari Nawawi, Pontianak, 78124, INDONESIA
2. Department of Chemistry, University of Leicester, University Road, Leicester, LE1 7RH, UK
*mpl10@leicester.ac.uk

Abstract
A new potential zinc-responsive gadolinium DO3A-based MRI contrast agent has been synthesized containing a picolinate acid group as an active arm. To study the complex properties, its emissive europium analogue has been prepared as a model. Changes in absorption and emission properties were observed as well as in the hydration number of the complex in response to increasing concentration of zinc (II). Further examination of the gadolinium complex showed a high relaxivity. In addition, a 32% modulation of relaxivity was observed in response to added zinc (II) ion which is beneficial as a zinc-responsive MRI contrast agent.

Keywords: Contrast agent, MRI, relaxivity, zinc.

Introduction
Zn is the second most abundant transition-metal ion after iron in the human body.[1] It is present as a divalent ion and spreads around the human body either tightly bound in proteins or as mobile pools which exist in certain mammalian organs such as the brain (0.1–0.5 mM),[2] pancreas[3] and prostate[4] which are carefully regulated; the total concentration in the body is eight to twelve times higher than copper.[1] The significant role for zinc is as a structural cofactor in metalloproteins.[1] Many studies report its contribution to several biological processes in metabolism and it is involved in enzyme regulation,[5] gene expression,[1] apoptosis[6] and neural signal transmission.[7]

Zinc (II) along with other metals is present as a neurochemical factor in some proteins which is relevant to disease pathophysiology.[2] Thus, the abundance of Zn (II) inside the body can be an indicator related to health, the disruption of which is correlated with some diseases including diabetes, prostate,[4] epilepsy, amyotrophic lateral sclerosis, hypoxia-ischemia,[8] certain cancers,[5] and Parkinson's disease.[9] A high level of Zn (II) is also observed in Alzheimer's disease [The zinc (II) ions released during neuro transmission may induce galvanization of beta-amyloid (Aβ) plaques occurring in Alzheimer's disease][9] inside the plaques formed of patients. In contrast, prostate diseases and diabetes are linked to zinc deficiency.[10]

Magnetic resonance imaging (MRI) is a powerful method in modern clinical application which is able to detect the physiological changes that provide the information of actual conditions at the molecular or cellular level[11] by providing non-invasive anatomical structure in high resolution.[10] In order to get sufficient readable signal, a contrast agent is needed. A number of different responsive contrast agents have been developed recently including zinc activated Gd-DOTA-based contrast agents such as Gd-DOTAdiBPEN in which the relaxivity is enhanced by 20% from 5.0 to 6.0 $mM^{-1}s^{-1}$ (at 37°C and 23 MHz)[12] and a Gd-DO3A-based contrast agent containing an iminodiacetate active group for Zn (II) binding which increased relaxivity by 73% from 2.3 to 5.1 $mM^{-1}s^{-1}$ (at 37°C and 60 MHz),[13] both of them are selective for Zn (II) over Na(I), K(I), Ca(II) and Mg(II), but not Cu(II).

In addition, a Zn-responsive bimodal MRI and luminescence imaging probe (MRI/LI) was developed from Gd-DO3A-based contrast agent appended quinoline derivatives such as amidoquinoline[3] and 8-sulfonamidoquinoline.[14] These contrast agents increased the relaxivity and the fluorescence in response to Zn (II), in which the relaxivity increased from 4.2 to 6.6 mM^{-1} s^{-1} (57% enhancement at 25°C, 9.4 T) and from 3.8 to 5.9 mM^{-1} s^{-1} (55% enhancement at 25°C, 23 MHz), while the fluorescence amplitude increased 3-fold and 7-fold for amidoquinoline and 8-sulfonamidoquinoline respectively.

There are several strategies to design a metal responsive MRI contrast agent; however, most of them rely on manipulating the number of exchangeable inner-sphere water molecules.[15] In addition, water exchange rate and reduction in molecular tumbling (which corresponds to the coordination lifetime of inner-sphere waters) are considered as other mutual mechanisms. The water content manipulation can be performed from high to low water content or vice versa by coordination displacement. This is usually done by the active arm. This mechanism is likely to be favorable in the development of responsive contrast agents due to the lack of solubility barrier compared to using multimeric compounds.

There is a possibility of a small molecule contrast agent to have a low molecular tumbling such as Gd-DOTA-diBPEN, due to complexation with HSA.[12] Herein, we report a new zinc-activated DO3A-based MRI contrast agent containing picolinate triazole tridentate ligand as an active arm. The picolinate triazole group is expected to be a good zinc chelator. Displacement of picolinate triazole from the central lanthanide to zinc is expected to allow more coordination of inner-sphere waters, thus increasing the proton relaxivity.

Material and Methods
Material: All solvents used were in high purity and purchased from commercially available sources without any

further purification unless otherwise stated, with the exception of water, which was obtained from Millipore purification system. All chemicals and starting materials were purchased either from Aldrich, Acros or Alfa.

General method: NMR spectra were recorded on a Bruker DRX400 MHz spectrometer at 298K and the chemical shifts are quoted in ppm relative to tetramethylsilane. Semi-preparative HPLC was conducted on a ThermoFisher Ultimate 3000 with chromeleon software on Phenomenex Luna C18 column. Absorption spectra were obtained from a Shimadzu UV-1024PC spectrometer using a 1 x 1 cm quartz Hellma cuvette. Luminescence spectra were recorded using a Jobin Yvon Horiba FluorMax-3 spectrometer in a 1 x 1 cm quartz Hellma cuvette. High resolution mass spectra were analysed on a Water Acquity XEVO Q ToF spectrometer or Applied Biosciences Voyager DE-STR MALDI TOF spectrometer and measured in *m/z*.

Caution: Low molecular weight organic azides were not isolated due to their explosive potential.

HPLC purification: Preparative and analytical reverse-phase HPLC were conducted by using a method as follows: 5% B for 5 min, 5-100 % B over 30 min, 100% B for 5 min, 100-5 % B over 5 min, 5 % B for 5 min. (Solvent A 0.1 % TFA in H_2O or 100% H_2O and solvent B 0.1% TFA in MeCN or 100 % MeCN).

Luminescence spectra measurements: The luminescence spectra and lifetime measurement of Ln.13 were recorded in aqueous 50 mM HEPES buffer pH / pD 7.4 at constant ionic strength (0.1 M NaCl). Ln.13 was excited at 292 nm and monitored at 617 nm during the lifetime studies. The slit widths were 5 and 1 nm for excitation and emission. The metal titrations were conducted by addition of standard free-metal solution gradually (5 µL aliquots) to achieve the sufficient equivalent concentration to 3 mL Ln.13 61.9 µM solution. The total volume changes were no more than 10%.

Relaxation-time measurements: Longitudinal relaxation time (T_1) of Gd.13 for both in the absence and presence of free-metal was measured at 298K, 400 MHz, 9.4 T (Bruker AV-400 NMR). Gd.13 1 mM was prepared by dissolving it in 10 mL of 1 % tert-butyl alcohol in 50 mM HEPES buffer solution containing 0.1 M NaCl, pH 7.4. Its exact concentration was measured by Evan's method in a co-axial capillary tube placed inside the 5 mm NMR sample tube comprising 1% tert-butyl alcohol in D_2O.[16] The relaxation time values were calculated from 16 points generated via standard inversion-recovery procedure which is fit by the equation 1 to give T_1 value and its relaxivity (r_1) was determined by using equation 2.

$$M_z = M_0\left[1 - 2\,exp\left(\frac{-\tau}{T_1}\right)\right] \quad (1)$$

where Mz = magnetization, Mo = magnetization, τ = time delay and T_1 = longitudinal relaxation (s).

$$r_1 = \frac{\left(\frac{1}{T_1}\right) - 0.4}{[Gd]} \quad (2)$$

where r_1 = relaxivity ($mM^{-1}\ s^{-1}$), [Gd] = concentration of Gd.13 (mM) and 0.4 = diamagnetic contribution of H_2O.

Synthesis of ethyl 6-bromopicolinate (2): 6-bromopicolinic acid (1) (1.102 g, 5.455 mmol) was dissolved in absolute ethanol and 4 drops of concentrated H_2SO_4 were then added. The reaction mixture was heated at reflux for 18 h. The solvent was removed in *vacuo*, then the residue was dissolved in 30mL DCM and washed (2 x 10 mL) with 1M $NaHCO_3$ solution. The organic layer was dried with $MgSO_4$, filtered and the solvent was removed in *vacuo* to give a white-brown solid.

Purification via column chromatography (SiO_2 EtOAc 100%) gave a white solid (1.157 g, 92%). ^{1}H NMR ($CDCl_3$, 400 MHz) δ 8.08 (1H, dd, *J* = 7.0, 1.6 Hz, ~CH-CH-C*H*~), 7.73 – 7.65 (2H, m, ~C*H*-C*H*-CH~), 4.47 (2H, q, *J* = 7.2 Hz, ~C*H*$_2$-CH$_3$), 1.43 (3H, t, *J* = 7.2 Hz, ~CH$_2$-C*H*$_3$); ^{13}C NMR ($CDCl_3$, 100 MHz) δ 164.0 (~COO~), 149.3 (~*C*-COO~), 142.3 (Br-*C*~), 139.2 (~CH-*C*H-CH~), 131.8 (~*C*H-CH-CH~), 124.1 (~CH-CH-*C*H~), 62.4 (~*C*H$_2$-CH$_3$), 14.4 (~CH$_2$-*C*H$_3$). *m/z* (ESMS$^+$) 229.9809 (calc. for $C_8H_9NO_2{}^{79}Br$ 229.9817) $[M+H]^+$.

Synthesis of ethyl 6-((trimethylsilyl)ethynyl) picolinate (3): Ethyl 6-bromopicolinate (2) (0.089 g, 0.389 mmol), $Pd(PPh_3)_2Cl_2$ (10.0 mg, 150 µmol) and CuI (3.0 mg, 150 µmol) were dissolved in 10 mL triethylamine under N_2. To the reaction mixture ethynyltrimethylsilane (0.152 g, 1.556 mmol) was then added dropwise via a syringe. After heating at 50 °C for 90 min, the reaction was showing to complete by TLC (SiO_2, EtOAc 100%, Rf = 0.75). To the reaction mixture, diethyl ether (30 mL) was then added followed by washing with 20 mL saturated NH_4Cl solution three times. The organic layer was dried with $MgSO_4$, filtered and the solvent was removed in *vacuo* to give a black solid.

Purification via column chromatography (SiO_2, DCM 100%) gave a brown-black solid (72 mg, 75 %). ^{1}H NMR ($CDCl_3$, 400 MHz) δ 8.04 (1H, dd, *J* = 7.8, 1.2 Hz, ~CH-CH-C*H*~), 7.80 (1H, t, *J* = 7.8 Hz, ~CH-C*H*-CH~), 7.62 (1H, dd, *J* = 7.8, 1.2 Hz, ~C*H*-CH-CH~), 4.47 (2H, q, *J* = 7.1 Hz, ~C*H*$_2$-CH$_3$), 1.44 (3H, t, *J* = 7.1 Hz, ~CH$_2$-C*H*$_3$), 0.27 (9H, s, ~Si(C*H*$_3$)$_3$; ^{13}C NMR ($CDCl_3$, 100 MHz) δ 164.8 (~*C*OO~), 148.7 (~*C*-COO~), 143.4 (~C≡*C*-*C*~), 137.1 (~CH-*C*H-CH~), 130.5 (~*C*H-CH-CH~), 124.2 (~CH-CH-*C*H~), 103.0 (~C≡*C*~), 96.3 (~*C*≡C~), 62.1 (~*C*H$_2$-CH$_3$), 14.3 (~CH$_2$-*C*H$_3$), -0.3 (~Si(*C*H$_3$)$_3$). *m/z* (ESMS$^+$) 248.1107 (calc. for $C_{13}H_{18}NO_2{}^{28}Si$ 248.1107) $[M+H]^+$.

Synthesis of ethyl 6-ethynylpicolinate (6): To a solution of (3) (195 mg, 0.788 mmol) in 10 mL THF was added TBAF (0.313 g, 1.200 mmol). The solution was then stirred at a room temperature for 1 h. The reaction completion was

monitored by TLC (SiO_2, EtOAc 100%, Rf = 0.66). The reaction mixture was concentrated.

Purification via SiO_2 column chromatography (EtOAc 100%) gave a brown solid (108 mg, 78%). ^{1}H NMR ($CDCl_3$, 400 MHz) δ 8.09 (1H, dd, *J* = 7.8, 1.0 Hz, ~CH-CH-C*H*~), 7.82 (1H, t, *J* = 7.8 Hz, ~CH-C*H*-CH~), 7.64 (1H, dd, *J* = 7.8, 1.0 Hz, ~C*H*-CH-CH~), 4.48 (2H, q, *J* = 7.2 Hz, ~C*H*$_2$-CH$_3$), 3.20 (1H, s, *H*C=C~), 1.44 (3H, t, *J*=7.2 Hz, ~CH$_2$-C*H*$_3$); ^{13}C NMR ($CDCl_3$, 100 MHz) δ 164.8 (~*C*OO~), 149.0 (~*C*-COO~), 142.7 (HC≡C-*C*~), 137.4 (~CH-*C*H-CH~), 130.5 (~*C*H-CH-CH~), 124.7 (~CH-CH-*C*H~), 82.2 (HC≡*C*~), 78.6 (H*C*≡C~), 62.3 (~*C*H$_2$-CH$_3$), 14.4 (~CH$_2$-*C*H$_3$). *m/z* (ESMS$^+$) 176.0712 (calc. for $C_{10}H_{10}NO_2$ 176.0712) [M+H]$^+$. *Synthesis of ethyl 6-(1-(3-hydroxypropyl)-1H-1,2,3-triazol-4-yl)picolinate* (7).

3-bromopropanol (4) (0.213 g, 1.53 mmol) and sodium azide (0.109 g, 1.68 mmol) were dissolved in 10 mL EtOH : H_2O (7:3). After heated at reflux for 18 h, the mixture was cooled to room temperature. Compound 6 (0.267 g, 1.52 mmol) followed by $CuSO_4.5H_2O$ (38.0 mg, 152 µmol) and sodium ascorbate (0.151 g, 0.763 mmol) were then added. After stirring at a room temperature for 18 h, the reaction completion was confirmed by TLC. The reaction mixture was then poured into saturated EDTA solution (made pH 10 by ammonia) before extracted by 20 mL ethyl acetate 3 times. The combined organic solvent was dried with $MgSO_4$, filtered and concentrated in *vacuo*.

Purification via SiO_2 column chromatography (EtOAc 100%) gave a yellow solid (0.253 g, 60%). ^{1}H NMR ($CDCl_3$, 400 MHz) δ 8.46 (1H, s, (~N-C*H*-C~ *triazole*), 8.36 (1H, dd, *J* = 7.9, 1.1 Hz, ~C*H*-CH-CH~), 8.03 (1H, dd, *J* = 7.8, 1.2 Hz, ~CH-CH-C*H*~), 7.92 (1H, t, *J* = 7.8 Hz, ~CH-C*H*-CH~), 4.62 (2H, t, *J* = 6.8 Hz, ~N-C*H*$_2$-CH$_2$~), 4.48 (2H, q, *J* = 7.2 Hz, ~O-C*H*$_2$-CH$_3$), 3.71 (2H, br t, *J* = 5.5 Hz, ~C*H*$_2$-OH), 2.63 (1H, br s, ~O*H*), 2.21 (2H, quin, *J* = 6.3 Hz, ~C*H*$_2$-CH$_2$-OH), 1.45 (3H, t, *J* = 7.2 Hz, ~O-CH$_2$-C*H*$_3$); ^{13}C NMR ($CDCl_3$, 100 MHz) δ 165.2 (~*C*OO~), 151.0 (~*C*-COO~),148.0 (~*C*-N-C~), 147.7 (~N-CH-*C*-C~), 138.0 (~CH-*C*H-CH~), 124.1 (~*C*H-CH-CH~), 123.7 (~N-*C*H-C~), 123.5 (~CH-CH-*C*H~), 62.1 (~O-*C*H$_2$-CH$_3$), 58.7 (~CH$_2$-OH), 47.3 (~N-*C*H$_2$-CH$_2$~), 32.7 (~*C*H$_2$-CH$_2$-OH), 14.4 (~O-CH$_2$-*C*H$_3$). *m/z* (ESMS$^+$) 277.1313 (calc. for $C_{13}H_{17}N_4O_3$ 277.1301) [M+H]$^+$.

Synthesis of ethyl 6-(1-(3-chloropropyl)-1H-1,2,3-triazol-4-yl)picolinate (8): Compound (7) (0.463 g, 1.68 mmol) was dissolved in dichloromethane. It was cooled in an ice bath under N_2. Thionyl chloride (0.798 g, 6.71 mmol) was then added via syringe, it was stirred for a while before the temperature was then allowed to increase to room temperature. The reaction mixture was stirred for 18 h. It was then poured into 10 mL $NaHCO_3$ 1M solution before extracted by 10 mL DCM three times. The combined organic solvent was dried with $MgSO_4$, filtered and the solvent was removed in *vacuo* to give a yellow-oily product.

Purification via column chromatography (SiO_2, EtOAc 100%) gave a white-yellow solid (0.395 g, 80%). ^{1}H NMR ($CDCl_3$, 400 MHz) δ 8.45-8.29 (2H, m, (~N-C*H*-C~ *triazole* and ~C*H*-CH-CH~), 8.04 (1H, d, *J* = 7.6 Hz, ~CH-CH-C*H*~), 7.93 (1H, t, *J* = 7.6 Hz, ~CH-C*H*-CH~), 4.64 (2H, t, *J* = 6.6 Hz, ~N-C*H*$_2$-CH$_2$~), 4.48 (2H, q, *J* = 7.0 Hz, ~O-C*H*$_2$-CH$_3$), 3.58 (2H, t, *J* = 6.0 Hz, ~C*H*$_2$-Cl), 2.46 (2H, quin, *J* = 6.1 Hz, ~C*H*$_2$-CH$_2$-Cl), 1.45 (3H, t, *J* = 7.0 Hz, ~O-CH$_2$-C*H*$_3$); ^{13}C NMR ($CDCl_3$, 100 MHz) δ 165.2 (~*C*OO~), 150.7 (~*C*-COO~), 148.1 (~*C*-N-C~), 147.9 (~N-CH-*C*-C~), 138.0 (~CH-*C*H-CH~), 124.2 (~*C*H-CH-CH~), 123.5 (~CH-CH-*C*H~), 123.4 (~N-*C*H-C~), 62.0 (~O-*C*H$_2$-CH$_3$), 47.5 (~N-*C*H$_2$-CH$_2$~), 41.1 (~*C*H$_2$-Cl), 32.7 (~*C*H$_2$-CH$_2$-OH),14.4 (~O-CH$_2$-*C*H$_3$). *m/z* (ESMS$^+$) 295.0963 (calc. for $C_{13}H_{16}N_4O_2{}^{35}Cl$ 295.0962) [M+H]$^+$.

Synthesis of tri-tert-butyl 2,2',2''-(1,4,7,10-tetraazacyclododecane-1,4,7-triyl) triacetate hydrobromide (10) by following a patent procedure[17]: Cyclen (9) (1.116 g, 6.594 mmol) and sodium acetate (1.622 g, 19.780 mmol) were dissolved in 15 mL dimethylacetamide at 0 ^{o}C. *tert*-butylbromoacetate (3.859 g, 19.783 mmol) in 2.5 mL dimethylacetamide was added drop-wise. After addition, the temperature was allowed to increase to room temperature and the reaction mixture was closed, sealed and stirred for 4 days. The reaction mixture was poured into 35 mL warm water (50 ^{0}C) containing potassium bromide (1.137g, 9.554 mmol) to give a pale-yellow solution. The pH was adjusted to 9 by the addition of solid sodium hydrogen carbonate to produce white suspension and it was left without stirring for 4 h.

It was filtered and dried to give a white solid (2.145 g, 55 %). ^{1}H NMR (400 MHz, $CDCl_3$), δ 9.96 (2H, br s, -N*H*-), 3.39 (4H, br s, ~C*H*$_2$-COO~), 3.30 (2H, br s, ~C*H*$_2$-COO~), 3.07-3.15 (4H, br, ring H), 2.92 (6H, br, ring H), 2.88 (6H, br, ring H), 1.46 (18H, br s, C*H*$_3$), 1.45 (9H, br s, C*H*$_3$); ^{13}C NMR (100 MHz, $CDCl_3$) δ 170.83, 170.23 (~*C*OO~), 81.7, 81.5, 81.28 (~*C*(CH$_3$)$_3$), 58.0 (~NCH$_2$COO~), 51.2, 49.1, 48.8, 47.4 (~NCH$_2$), 28.1 (~C(*C*H$_3$)$_3$); *m/z* (ESMS+) 515.3817 (calc. for $C_{26}H_{51}N_4O_6$ 515.3809) [M+H]$^+$.

Synthesis of tri-tert-butyl 2,2',2''-(10-(3-(4-(6-(ethoxycarbonyl)pyridin-2-yl)-1H-1,2,3-triazol-1-yl) propyl)-1,4,7,10-tetraazacyclododecane-1,4,7-triyl) triacetate (11): Compound (10) (0.439 g, 0.737 mmol) along with K_2CO_3 (0.407 g, 2.948 mmol) were placed in a two-neck rbf. It was degassed before compound (8) (0.239 g, 0.810 mmol) in 15 mL dry MeCN (dried using a PureSolv solvent drying system from Innovative Technologies) was then added via syringe. After heating at reflux for 18h, the reaction mixture was poured into 10 mL 1M $NaHCO_3$ solution and was extracted by DCM three times. The combined organic layer was dried with $MgSO_4$ before concentrated in *vacuo* to give a brown oily product.

Purification via SiO_2 column chromatography (DCM:MeOH 9:1) gave a light-yellow oily product (0.484 g, 85%). ^{1}H

NMR (400 MHz, CHLOROFORM-*d*) δ ppm 8.50 (1H, s, (~N-C*H*-C~ *triazole*), 8.33 (1H, dd, *J*=7.8, 1.2 Hz, ~C*H*-CH-CH~), 8.03 (1H, dd, *J*=7.8, 1.0 Hz, ~CH-CH-C*H*~), 7.93 (1H, t, *J*=7.8 Hz, ~CH-C*H*-CH~), 4.40 - 4.55 (4H, m, ~CH_2-N-N-N~; ~O-CH_2-CH_3), 2.06 - 3.29 (26H, m, ~CH_2COO~; ~N-CH_2-CH_2-N~; ~CH_2-CH_2-CH_2-N~), 1.34 - 1.56 (30H, m, ~C(CH_3)$_3$~; ~O-CH_2-CH_3); ^{13}C NMR (101 MHz, $CDCl_3$) δ ppm 173.6, 172.6 (~*C*OOC(CH_3)$_3$~), 165.1 (~*C*OOCH_2CH_3), 150.6 (~*C*-COOCH_2CH_3~), 147.9, 147.5 (~N-N-N-*C*-*C*-N~), 137.8 (~CH-*C*H-CH~), 124.0 (~CH-CH-*C*H~), 123.3 (~*C*H-CH-CH~) & (~N-*C*H-C~ triazole), 82.9, 82.5 (~*C*-(CH_3)$_3$), 61.9 (~COO*C*H_2CH_3), 58.0 – 50.2 (~N*C*H_2COO~), (~*C*$H_2CH_2CH_2$NNN~) & (~N*C*H_2), 48.9 (~CH_2CH_2*C*H_2NNN~), 27.9, 27.8 (~C(*C*H_3)$_3$), 26.7 (~CH_2*C*H_2CH_2NNN~), 14.3 (~COOCH_2*C*H_3). *m/z* (ESMS$^+$) 773.4920 (calc. for $C_{39}H_{65}N_8O_8$ 773.4925) $[M+H]^+$.

Synthesis of 2,2',2''-(10-(3-(4-(6-(ethoxycarbonyl) pyridin-2-yl)-1H-1,2,3-triazol-1-yl)propyl)-1,4,7,10-tetraazacyclododecane-1,4,7-triyl) triacetic acid (12): To a solution of compound (11) (0.101 g, 130.6 mmol) in 5 mL DCM, 5 mL TFA was added. After stirring at room temperature under open atmosphere for 18h, the solvent was removed in *vacuo*. To wash the residue, 30 mL DCM was added and it was dried in *vacuo*. This washing process was repeated three times with DCM and once with diethyl ether to give a brown oily product.

Purification *via* HPLC (Rt 20.1 min) gave a white solid (73 mg, 92%). ^{1}H NMR (400 MHz, METHANOL-d_4) δ ppm 8.68 (1H, s, ~N-C*H*~ *triazole*), 8.25 (1H, dd, *J*=6.3, 2.9 Hz, ~C*H*-CH-CH~), 8.00 - 8.12 (2H, m, ~CH-C*H*-C*H*~), 4.64 (2H, t, *J*=6.8 Hz, ~CH_2-CH_2-CH_2~), 4.47 (2H, q, *J*=7.2 Hz, ~O-CH_2-CH_3), 4.15 (2H, br s, ~CH_2-COOH), 3.34 - 3.81 (14H, m, ~N-CH_2-CH_2-N-CH_2-CH_2-N~; ~CH_2-COOH; ~CH_2-COOH; ~N-CH_2-CH_2-CH_2~), 2.90 - 3.27 (8H, m, ~N-CH_2-CH_2-N-CH_2-CH_2-N~), 2.46 - 2.62 (2H, m, ~N-CH_2-CH_2-CH_2~), 1.44 (t, *J*=7.2 Hz, ~O-CH_2-CH_3). ^{13}C NMR (101 MHz, METHANOL-d_4) δ ppm 174.6 (~*C*OOH), 166.5 (~*C*OOC_2H_5), 151.7 (~*C*-$COOC_2H_5$), 149.1 (~*C*-N-C-$COOC_2H_5$), 148.6 (~N-N-N-*C*~), 139.8 (~CH-*C*H-CH~), 125.4 (~N-*C*H~ *triazole*), 125.3 (~CH-CH-*C*H~), 124.5 (~*C*H-CH-CH~), 63.2 (~O-*C*H_2-CH_3), 55.6, 53.7 (~*C*H_2-COOH), 53.2, 52.7, 51.3, 50.1 (~N-*C*H_2-*C*H_2-N~ ring), 49.8, (~*C*H_2-CH_2-CH_2~), 48.8 (~CH_2-CH_2-*C*H_2~), 25.9 (~CH_2-*C*H_2-CH_2~), 14.5 (~O-CH_2-*C*H_3). *m/z* (ESMS$^+$) 605.3069 (calc. for $C_{27}H_{41}N_8O_8$ 605.3047) $[M+H]^+$.

Synthesis of Europium and Gadolinium complex (Ln.13): To a solution of 12 (50 mg, 82.689 µmol) in 10 mL H_2O, $EuCl_3.6H_2O$ (30 mg, 84.606 µmol) or $GdCl_3.6H_2O$ (31 mg, 83.402 µmol) was added. The pH was adjusted to 6.4 with 0.1M HCl. The mixture was heated at reflux for 18h. It was cooled and the pH was adjusted to 10 by 0.1M NaOH then filtered through celite. It was reheated at reflux for 18h. The pH was returned back to 7 by HCl 0.1 M. The absence of free Ln(III) was confirmed by xylenol orange test. After freeze-drying purification via HPLC (Rt 17.6 min) gave a white solid containing NaCl (65 mg / 108% (Eu.13); 69 mg / 115% (Gd.13)). *m/z* (MALDI-TOF) 732.1641 (calc. $C_{25}H_{34}N_8O_8{}^{157}$Gd 732.1741) for Gd.13 $[M+2H]^+$; 727.2058 (calc. $C_{25}H_{34}N_8O_8{}^{152}$Eu 727.1712) for Eu.13 $[M+2H]^+$

Results and Discussion

The design of Gd.13 as a new zinc-responsive gadolinium-based MRI contrast agent uses a well-known high stability chelator the macrocycle ligand DO3A, which is attached by an exchangeable coordinated arm, this 'active arm' contains a picolinate triazole moiety. It has been agreed that the use of a cyclic chelate is beneficial in terms of high thermodynamic and kinetic stabilities, reducing the probability of lanthanide decomplexation.[18] Furthermore, it also reported that it has a high water-exchange rate[19] which means more water can be relaxed and therefore suited as a contrast agent chelator.

The responsive DO3A-based probe relies on the fourth arm / active arm containing specific ligands which can bind either to the coordination site of lanthanide and/or with the activator such as metal ion, enzyme etc. Here we report the exploitation of picolinate triazole ligand to provide such conformation which can form a linear tridentate ligand, which is favorable for mer-octahedral conformation (as with zinc). In addition, the carboxylic acid group has a good charge interaction with the lanthanide to maintain its stability.

A number of synthesis routes were attempted to give the best reaction pathway as depicted at scheme 1 and scheme 2. The title compound (Ln.13) was synthesized in twelve steps and was fully characterized, including all intermediate compounds. It was started by two main starting materials cyclen (9) and 6-bromo picolinic acid (1). In order to aid purification throughout the various steps on the carboxylic compound as in compound 1, it was converted to the ethyl ester form of picolinic acid (compound 2) which was relatively easy to handle for the subsequent synthesis steps. It was synthesized through the common acid-catalysed esterification reaction procedure in high yield.

Sonoghasira coupling of (2) was conducted using the reaction conditions described by D'Amora et al[20] without any modification to give (3). Tetrabutylammonium fluoride was preferred to remove the trimethylsilyl group, to give (6) as potassium carbonate resulted in ethyl ester hydrolysis. Compound (7) was synthesized through a common copper(I) catalyzed azide-alkyne cycloaddition reaction. In this case, isolation of potentially explosive organic azide (5) was avoided, it was generated *in situ* by reacting bromo propanol (4) with sodium azide followed by the addition of (6) and the copper catalyst.

The pendant arm was then introduced to the macrocycle by first activating the oxygen atom with a chloride leaving group followed by reaction with the DO3A precursor (10). Finally, acid hydrolysis of the *tert*-butyl ester generated the

proligand (12). Complexation with Eu(III) and Gd(III) was achieved by controlling the pH at ~ 6.4 and strictly maintaining acidic conditions to minimize any ethyl ester hydrolysis. To maintain the ester form is crucial in this stage to prevent any lanthanide complexation by the tridentate pendant arm.

To study the properties of the Gd(III) complex, the analogue Eu(III) complex (Eu.13) was synthesized. This complex can give information of Gd.13 by studying its photophysical properties such as its characteristic emission spectrum or the emission lifetime. The clues to the coordination environment of the entire complex can be gained via these studies. Furthermore, the emission pattern or the emission transformation gave important information when investigating the behavior of probe in response to the presence of Zn (II). The picolinate triazole moiety in compound Eu.13 not only acts as an active coordination arm, but it also behaves as an antenna (sensitizer) which can capture energy in the form of light and transfer it to the europium center.

This sensitizing mechanism of europium excitation takes place through a triplet state pathway which is long-lived state due to spin forbidden transition, allowing energy transfer to excite Eu(III) from its electronic ground state. This mechanism is more effective compared to direct excitation, especially for Eu(III) as it possesses a relatively low extinction coefficient. The energy transfer process itself is distance dependent, the length of the carbon linker to the macrocycle significantly changes the energy transfer efficiency from the antenna to the europium.

Increasing the number of methylenes on the linker, increases the distance and therefore energy transfer is less efficient ($1/r^6$ dependency) and emission is less intense. Coordination of picolinate triazole trough the carboxylic site to the europium, shortens the distance, therefore maintains the efficiency of energy transfer.

The spectra of Gd.13 (figure 1.A), show the excitation (dash line) and fluorescence emission (solid line) of the picolinate triazole moiety with a maximum emission peak at 361 nm and excitation maxima at 292 nm. Emission from the picolinate triazole moiety is absent in Eu.13 (figure 1.B), indicating the occurrence of energy transfer from the picolinate triazole moiety to europium. The energy received by the europium gives rise to a luminescent emission characteristic of europium.

The luminescent emission of compound Eu.13 contains five major emission peaks from main electron transition namely ΔJ = 0, 1, 2, 3, 4 at 579, 590, 616, 649, 689 nm respectively. The intensity of ΔJ = 1 (which corresponds to $^5D_0$-$^7F_1$) is significantly lower than ΔJ = 2 (corresponding to $^5D_0$-$^7F_2$), this is characteristic for 8-site coordination by a DO3A-based complex.[21]

Through this emissive europium complex analogue, the most crucial information relevant to an MRI contrast agent (of the corresponding Gd(III) complex) is the hydration state (*q*); this can be readily obtained.

It can be calculated by measuring the luminescent lifetime of Eu.13 in two different solvents H_2O and D_2O. The decay constant of the europium complex in deuterated water is smaller than in the normal water due to less efficient energy transfer experienced from emissive state of europium to the higher vibration energy level of D_2O (vibration energy level v = 4) compared to H_2O (vibration energy level v = 3), so its emission is quenched less.[22]

Using these decay constants, the *q* value can be determined using equation 3.[23] The lifetime studies of Eu.13 indicate that *q* = 0.8 ($\pm$ 0.2) at 298K (50 mM HEPES buffer pH 7.4 containing 0.1M NaCl) confirming 8-site coordination (the four macrocycle nitrogens, three carboxylate oxygens of DO3A plus an additional donor from the pendant arm).

$$q = 1.2\left(k_{H_2O} - k_{D_2O} - 0.25\right) \quad (3)$$

where *q* = hydration number, k_{H2O} = decay constant in H_2O and k_{D2O} = decay constant in D_2O.

Addition of zinc (II) increased the emission intensity of the picolinate triazole moiety of Gd.13 at 354 nm. The zinc (II) titration was carried out in 50 mM HEPES buffer pH 7.4 over a constant ionic strength (NaCl 0.1M). The emission of the picolinate triazole moiety increased 128% on addition of 1 equivalent of zinc (II), increasing by 188% after 6 equivalents of zinc (II) were added (figure 2A). The fluorescence amplitude revealed relatively little change in the presence of some other metals such as Fe^{2+}, Fe^{3+} and Ca^{2+}. In contrast, the emission intensity was diminished in response to Cu^{2+} (figure 3).

A coordination displacement of picolinate triazole from central lanthanide in Gd.13 upon the zinc titration is postulated, opening the pendant arm and brings it away from the central metal. This allows more waters to interact to the central lanthanide and to increase the relaxivity. The coordination displacement is indeed observed by the enhancement of picolinate triazole emission intensity in which the zinc binding obstructs the electron transfer deactivation processes in picolinate triazole moiety, similar to that observed in 8-sulfonamido quinoline.[14] The binding constant calculation (figure 2B) showed that the probe is tightly bound (K_d = 39.0 $\pm$ 3.1 μM) to the zinc(II) ion at physiological concentration.

The expected emission pattern was observed in Eu.13 during the metal titration. The picolinate triazole emission at 355 nm increased 574% from the initial intensity over the addition of 1 equivalent zinc (II) and even more over the subsequent additions (figure 4A). The emission behavior of Eu.13, during the zinc (II) titration however, is expected to provide more information to investigate the coordination

displacement, in which the sensitizing process is present in this complex. The enhancement of picolinate triazole emission at 355 nm was clearly understandable as in Gd.13. For Eu.13, the coordination displacement process is expected to increase the distance between the antenna and the central europium causing more inefficient energy transfer and therefore, it is anticipated that this will reduce the intensity of europium emission. This was observed by the experiment.

The emission intensity of europium gradually decreased in response to zinc (II) (Figure 4B). The coordination displacement of the picolinate triazole by zinc (II) ion is supported by lifetime studies. The hydration number of Eu.13 was calculated before and after the addition of zinc (II) ion as presented at table 1. The hydration number increased gradually from 0.80 (at the initial condition) to 1.27, 1.42, 1.58, 1.63 during the addition of 0.5, 1.0, 1.5, 2.0 equivalent of zinc (II) ion respectively. More addition of the zinc (II) ion to 2.5 equivalent maintains the hydration number at 1.63.

Relaxation measurements of Gd.13 (0.072 mM) were conducted by using a 9.4T NMR probe at 400 MHz at 298K in 50 mM HEPES buffer pH 7.4 over a constant ionic strength (NaCl 0.1 M). The r_1 relaxivity increased upon addition of Zn (II) and Cu(II), however it remained unchanged on addition of other biological relevant metal ions Ca(II), Fe(II) and Fe(II) (table 2). An unexpected high relaxivity value of 6.47 $mM^{-1}s^{-1}$ in the absence of free metal ion was observed. This is higher than typical q = 1 Gd.DOTA-based complexes (~ r_1 = 4.2 mM^{-1} s^{-1}).[24]

This could be due to the dimerization of the Gd.13 which has potential to occur at higher concentration reducing the molecular tumbling, although the tumbling effect is usually not significantly observed at 400 MHz. It also could be caused by ordered second-sphere water molecules around the pendant arm.

A significant increase in relaxivity was observed during zinc binding. r_1 increased as much as 29% and 32% during the addition of 0.5 and 1.0 equivalent zinc (II) respectively which was slightly higher than those with copper(II) (28%). Although it displays almost the same enhancement with copper, it is believed that this probe would not interfere significantly with copper since the concentration of Cu(II) in general is much lower than the concentration of Zn (II) inside the body,[1, 25] or in the specific organs such as pancreas[3] and prostate.[4]

In addition, these two metal ions are also found simultaneously in certain places such as in amyloid plaques and co-localized with the amyloide-β deposits, associated with Alzheimer's disease.[25] The relaxivity did not significantly change upon addition of zinc(II) from 0.5 to 1.0 equivalent, which could be an indication of 1:1 binding model. Mass spectrometric analysis of Gd.13-Zn (II) failed to prove this model, since electrospray ionization method used is not suitable for this compound. However, mass spectrometry data of free arm (7) and zinc (II) showed a peak at m/z 581 $[ZnL_2+Na]^+$ proving that two picolinate triazole ligands bound to one zinc(II) ion to form an octahedral conformation.

Table 1
The hydration number measurement of Eu.13 during Zn (II) addition in 50mM HEPES buffer pH/pD 7.4 containing 0.1M NaCl

Zn (II) equivalents	k_{H_2O}	k_{D_2O}	q (± 0.2)
0.0	1.55	0.63	0.80
0.5	1.90	0.58	1.27
1.0	2.01	0.59	1.42
1.5	2.12	0.56	1.58
2.0	2.17	0.56	1.63
2.5	2.20	0.58	1.63

Table 2
The relaxivity values of Gd.13 in response to several metal ions

Condition	Relaxivity (r_1) values of 0.7 mM Gd.13 over the addition free metal ion	
	0.5 equivalent	1.0 equivalent
Metal-free	6.47	
Zn^{2+}	8.38	8.56
Ca^{2+}	6.38	6.38
Fe^{2+}	6.34	n/a
Fe^{3+}	6.17	5.55
Cu^{2+}	8.45	8.33

Conclusion

In conclusion, here we report a new potential zinc (II)-responsive gadolinium DO3A-based MRI contrast agent containing an active arm picolinate triazole group (Gd.13). The initial examination on Gd.13 and its emissive europium complex Eu.13 showed a significant change on its emission spectra in response to the added zinc (II), which was indicating the occurrence of picolinate-coordination displacement from gadolinium center to zinc (II). This was verified by the hydration number study on Eu.13 which enhanced during zinc (II) addition.

The relaxivity measurement of Gd.13 exhibited a modulation of 29 to 32 % upon addition of 0.5 to 1.0 equivalent of zinc (II) ion, with a good selectivity over some other essential transition metals found inside the living organisms. We found that the zinc (II) binding constant value of Gd.13 (39.0 ± 3.1 μM) is in range of the actual zinc (II) concentration in several places inside the body which makes it reliable as a zinc(II)-responsive MRI contrast agent.

Acknowledgement

The authors thank to Dr. Gerry Griffith for NMR experiments, Mr. Mick Lee for mass spectroscopy analysis and Ministry of Research, Technology and Higher Education Directorate General of Resources for Research, Technology and Higher Education Republic of Indonesia for funding.

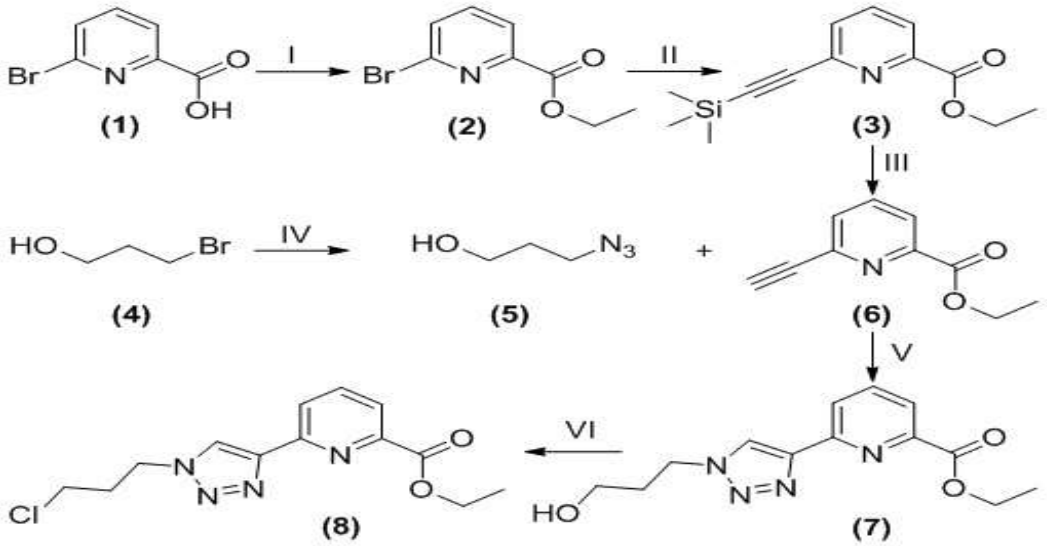

Scheme 1: Synthetic route to picolinic triazole arm (8). (I). Ethanol, H_2SO_4, reflux (90%). (II). Trimethylsilyl acetylene, CuI, Pd $(PPh_3)_2Cl_2$, Triethyl amine, 50 ^OC (75%). (III). TBAF, THF (90%). (IV). NaN_3, MeOH: H_2O 3:1, reflux. (V). $CuSO_4$, Na Ascorbate, MeOH: H_2O 3:1, 65^OC (60% 0ver two steps). (VI). $SOCl_2$, DCM, 0-25^OC (80%).

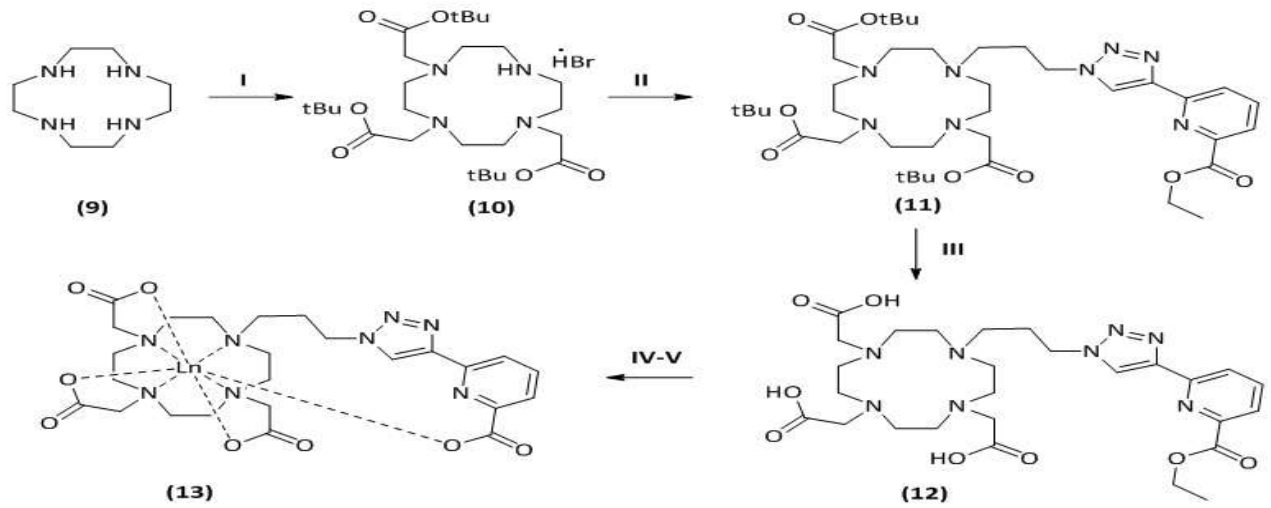

Scheme 2: Synthetic route to Ln.13. (I). t-Butyl bromoacetate, NaAcetate, DMA, 0-25 ^OC (75%). (II). 8, K_2CO_3, dry Acetonitrile, reflux (85%). (III). TFA: DCM 1:1, RT (70%). (IV). $EuCl_3.6H_2O$/ $GdCl_3.6H_2O$, H_2O, pH 6, 90 ^OC. (V). $NaOH_{(aq)}$, H_2O, 90 ^OC.

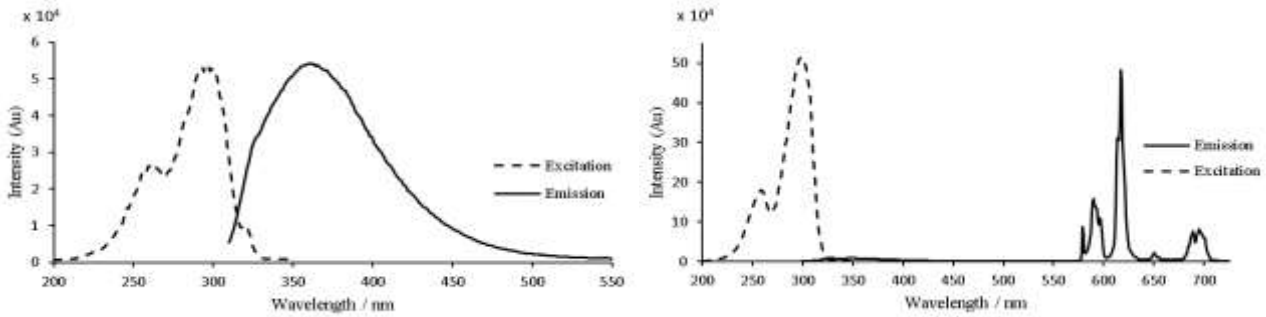

(**A**) (**B**)

Figure 1: Excitation (dash line) and emission (solid line) spectra of (A) Gd.13 (H_2O, pH 7.4, λ_{ex} = 292 nm, λ_{em} = 361 nm) and (B) Eu.13 (H_2O, pH 7.4, λ_{ex} = 292 nm, λ_{em} = 616 nm)

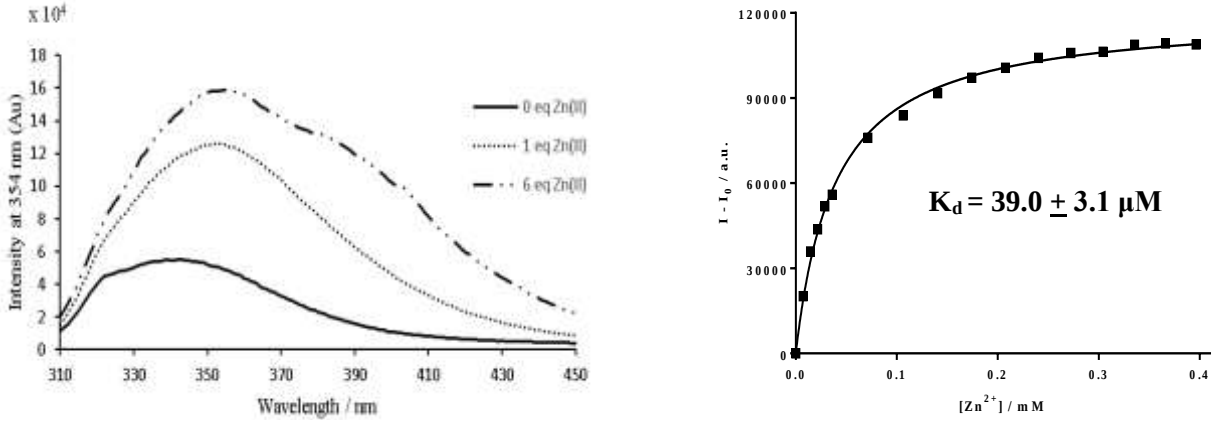

(A) **(B)**

Figure 2: (A) Emission profile of Gd.13 in response to zinc(II). (B) Fitting of 1:1 binding model of Gd.13 (72.7µM, 50mM HEPES buffer pH 7.4, 0.1M NaCl, H_2O, at 354 nm).

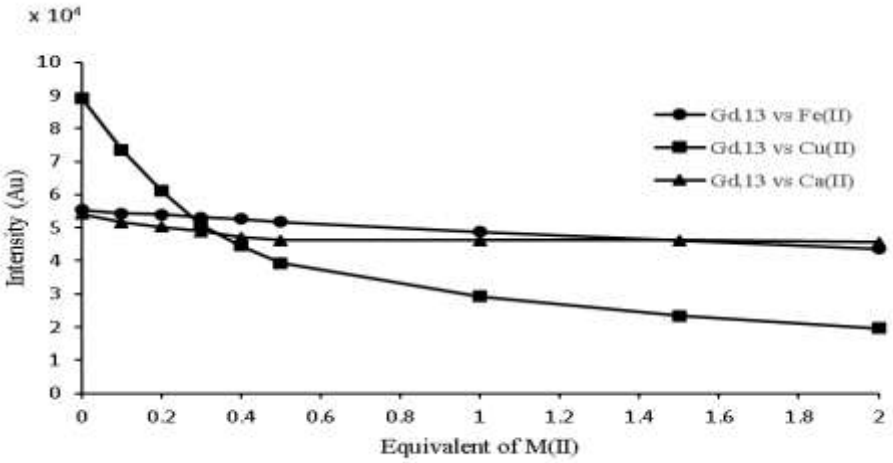

Figure 3: Emission intensity (340 nm) vs equivalents of M(II) for Gd.13 (72.7µM, 50mM HEPES buffer pH 7.4, 0.1M NaCl, H_2O).

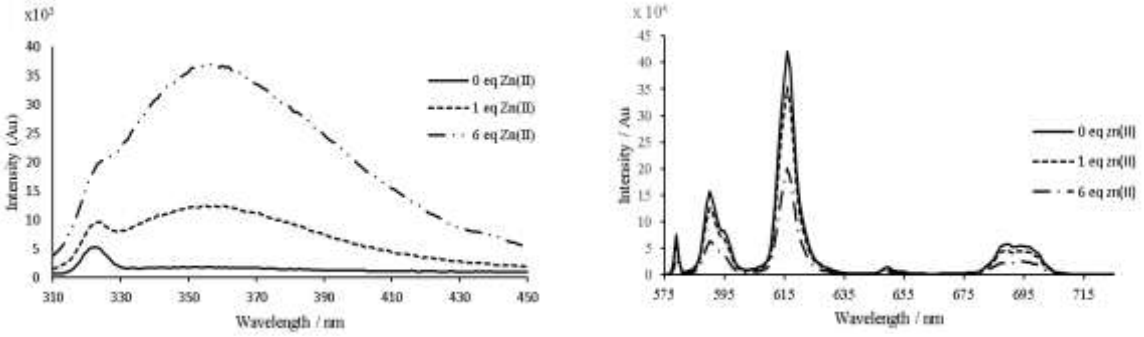

(A) **(B)**

Figure 4: Emission profile of (A) picolinate triazole moiety and (B) the europium center of Eu.13 in response to zinc(II) (50mM HEPES buffer pH 7.4, 0.1M NaCl, H_2O).

References

1. Jiang P. and Guo Z., Fluorescent detection of zinc in biological systems: Recent development on the design of chemosensors and biosensors, *Coord. Chem. Rev.*, **248**, 205–229 **(2004)**

2. Bush A.I., Metals and neuroscience, *Curr. Opin. Chem. Biol.*, **4**, 184–191 **(2000)**

3. Stasiuk G.J., Minuzzi F., Sae-Heng M., Rivas C., Juretschke H.P., Piemonti L., Allegrini P.R., Laurent D., Duckworth A.R., Beeby A., Rutter G.A. and Long N.J., Dual-Modal Magnetic Resonance/Fluorescent Zinc Probes for Pancreatic β-Cell Mass Imaging, *Chem.Eur. J.*, **21**, 5023–5033 **(2015)**

4. De Leon-Rodriguez L., Lubag A.J.M. and Dean Sherry A., Imaging free zinc levels in vivo - What can be learned?, *Inorg. Chim. Acta*, **393**, 12–23 **(2012)**

5. Hooper N.M., Families of zinc metalloproteases, *FEBS Lett.*, **354**, 1–6 **(1994)**

6. Kimura E., Aoki S., Kikuta E. and Koike T., A macrocyclic zinc(II) fluorophore as a detector of apoptosis, Proc. Natl. Acad. Sci. U. S. A., **100**, 3731–3736 **(2003)**

7. Takeda A., Zinc homeostasis and functions of zinc in the brain, *Bio Metals*, **14**, 343–351 **(2001)**

8. Cuajungco M.P. and Lees G.J., Zinc Metabolism in the Brain: Relevance to Human Neurodegenerative Disorders, *Neurobiol. Dis.*, **4**, 137–169 **(1997)**

9. Barnham K.J. and Bush A.I., Metals in Alzheimer's and Parkinson's Diseases, *Curr. Opin. Chem. Biol.*, **12**, 222–228 **(2008)**

10. Que E.L. and Chang C.J., Responsive magnetic resonance imaging contrast agents as chemical sensors for metals in biology and medicine, *Chem. Soc. Rev.*, **39**, 51–60 **(2010)**

11. Cakić N., Gündüz S., Rengarasu R. and Angelovski G., Synthetic strategies for preparation of cyclen-based MRI contrast agents, *Tetrahedron Lett.*, **56**, 759–765 **(2015)**

12. Esqueda A.C., Lopez J.A., Andreu-de-Riquer G., Alvarado-Monzon J.C., Ratnakar J., Lubag A.J.M., Sherry A.D. and Rodrıguez L.M.D., A new gadolinium-based MRI zinc sensor, *J. Am. Chem. Soc.*, **131**, 11387–11391 **(2009)**

13. Major J.L., Parigi G., Luchinat C. and Meade T.J., The synthesis and in vitro testing of a zinc-activated MRI contrast agent, Proc. Natl. Acad. Sci. U. S. A., **104**, 13881–13886 **(2007)**

14. Luo J., Li W.S., Xu P., Zhang L.Y. and Chen Z.N., Zn^{2+} responsive bimodal magnetic resonance imaging and fluorescent imaging probe based on a gadolinium(III) complex, *Inorg. Chem.*, **51**, 9508–16 **(2012)**

15. Bonnet C.S. and Tóth É., Smart MR imaging agents relevant to potential neurologic applications, *Am. J. Neuroradiol.*, **31**, 401–409 **(2010)**

16. Corsi D.M., Platas-Iglesias C., Van Bekkum H. and Peters J.A., Determination of paramagnetic lanthanide(III) concentrations from bulk magnetic susceptibility shifts in NMR spectra, *Magn. Reson. Chem.*, **39**, 723–726 **(2001)**

17. Axelsson O.H. and Olsson A.M., Synthesis of Cyclen Derivatives, US Patent 8, 138, 332 **(2012)**

18. Rashid H.U., Yu K. and Zhou J., Lanthanide(III) chelates as MRI contrast agents: A brief description, *J. Struct. Chem.*, **54**, 223–249 **(2013)**

19. Stasiuk G.J. and Lowe M.P., Click chemistry with lanthanide complexes: a word of caution, *Dalton Trans.*, 9725–9727 **(2009)**

20. D'Amora A., Fanfoni L., Cozzula D., Guidolin N., Zangrando N., Felluga F., Gladiali S., Benedetti F. and Milani B., Addressing the poly- to oligo-ketone selectivity in styrene carbonylation catalyzed by palladium/bpy complexes. effect of the 6-alkyl substitution, *Organometallics*, **29**, 4472–4485 **(2010)**

21. Jauregui M., Perry W.S., Allain C., Vidler L.R., Willis M.C., Kenwright A.M., Snaith J.S., Stasiuk G.J., Lowe M.P. and Faulkner S., Changing the local coordination environment in mono- and bi- nuclear lanthanide complexes through 'click' chemistry, *Dalton Trans.*, 6283 **(2009)**

22. Bruce J.I., Lowe M.P. and Parker D., Chapter 11 - Photophysical Aspects of Lanthanide(III) Complexes, In Merbach A.E. and Toth E., ed., The contrast agents in MRI, John Wiley and Sons, Ltd., Chichester **(2001)**

23. Beeby A., Clarkson I.M., Dickins R.S., Faulkner S., Parker D., Royle L., de Sousa A.S., Williams J.A.G. and Woods M., Non-radiative deactivation of the excited states of europium, terbium and ytterbium complexes by proximate energy-matched OH, NH and CH oscillators: an improved luminescence method for establishing solution hydration states, *J. Chem. Soc. Perkin Trans.*, **2**, 493–504 **(1999)**

24. Stasiuk G.J. and Long N.J., The ubiquitous DOTA and its derivatives: the impact of 1,4,7,10-tetraazacyclododecane-1,4,7,10-tetraacetic acid on biomedical imaging, *Chem. Commun.*, **49**, 2732 **(2013)**

25. Faller P. and Hureau C., Bioinorganic chemistry of copper and zinc ions coordinated to amyloid-β peptide, *Dalton Trans.*, 1080–1094 **(2009)**.